

MEASURING THE SPIN AND PARITY OF A RESONANCE IN THE $\gamma\gamma$ DECAY CHANNEL

WILCO J. DEN DUNNEN

Inst. for Theoretical Physics, Universität Tübingen, Auf der Morgenstelle 14, 72076 Tübingen, Germany

We present a way to determine the spin and parity of a resonance produced through gluon fusion with a decay to a $\gamma\gamma$ pair based on the transverse momentum and Collins-Soper ϕ distribution. This method also allows one to distinguish between various non-minimal coupling spin-2 scenarios and can be used in parallel to the ‘standard’ method based on the polar angle θ .

1 Introduction

In July 2012 the ATLAS and CMS collaborations announced the discovery of a new resonance^{1,2} in their search for the Standard Model (SM) Higgs boson. Decays of this resonance to ZZ ^{3,5} and $\gamma\gamma$ ³ have been established at over 5 sigma, whereas strong evidence ($\sim 4\sigma$) exists for a decay to WW ^{3,6}. Besides these channels, first measurements of the decay to $\tau\tau$ (3σ)⁷ and to bb (2σ)⁸ have now also been published.

Measurements of the spin of the resonance exclude a minimal coupling spin-2 resonance produced through gluon fusion in the ZZ channel at approximately 2σ ⁵. The same scenario is excluded at almost 3σ in the $\gamma\gamma$ channel³ and at 2σ in the WW channel³. Exclusions in the remaining channels or of non-minimal coupling spin-2 scenarios have not yet been presented.

Regarding the parity of the resonance, the option of a pseudoscalar in the ZZ channel has been excluded at approximately 2.5σ ³, whereas in the WW channel this can only be done at 1σ ⁶. In the $\gamma\gamma$ channel no parity determination can be made using conventional methods^{9,10,11,12,13} as the hard scattering $gg \rightarrow h \rightarrow \gamma\gamma$, which is characterized by only one single angle θ , is independent of the parity of h .

We will discuss here a method to determine both the parity of a resonance in the $\gamma\gamma$ channel¹⁴ and to distinguish between various spin-2 coupling scenarios that could not be distinguished on the basis of the θ distribution alone¹⁵. As we will show, various spin-2 scenarios can be distinguished on the basis of the Collins-Soper ϕ distribution, whereas the parity of the resonance manifests itself through the transverse momentum distribution. The effects on the transverse momentum distribution are small, but the effect on the ϕ distribution, for various spin-2 scenarios, is large enough to be measurable with the currently recorded data set.

The underlying principle of these methods relies on the fact that gluons are linearly polarized in the direction of their transverse momentum when entering the hard scattering. This polarization can be generated perturbatively, but it can also have a non-perturbative (intrinsic) component. It was realized that the perturbatively generated polarization forces one to modify the standard (quark initiated) Drell-Yan q_T -resummation procedure^{16,17} and its effects on SM Higgs boson production have since been taken into account^{18,19,20,21}. We will employ Transverse Momentum Dependent (TMD) factorization to systematically take into account both pertur-

bative *and* non-perturbative gluon polarization and calculate the effect on arbitrary colorless spin-0 and spin-2 boson production.

2 The $pp \rightarrow X_{0,2}X \rightarrow \gamma\gamma X$ differential cross section in TMD factorization

Within TMD factorization the full $pp \rightarrow X_{0,2}X \rightarrow \gamma\gamma X$ cross section, for a gluon fusion initiated process, is split into a partonic $gg \rightarrow \gamma\gamma$ cross section and two TMD gluon correlators that describe the distribution of gluons inside the proton as a function of their longitudinal and transverse momentum. More specifically, the differential cross section is written as^{22,23,24},

$$\frac{d\sigma}{d^4q d\Omega} \propto \int d^2\mathbf{p}_T d^2\mathbf{k}_T \delta^2(\mathbf{p}_T + \mathbf{k}_T - \mathbf{q}_T) \mathcal{M}_{\mu\rho} (\mathcal{M}_{\nu\sigma})^* \Phi_g^{\mu\nu}(x_1, \mathbf{p}_T, \zeta_1, \mu) \Phi_g^{\rho\sigma}(x_2, \mathbf{k}_T, \zeta_2, \mu), \quad (1)$$

with the longitudinal momentum fractions $x_1 = q \cdot P_2 / P_1 \cdot P_2$ and $x_2 = q \cdot P_1 / P_1 \cdot P_2$, q the momentum of the photon pair, \mathcal{M} the $gg \rightarrow \gamma\gamma$ partonic hard scattering matrix element and Φ the following gluon TMD correlator in an unpolarized proton,

$$\begin{aligned} \Phi_g^{\mu\nu}(x, \mathbf{p}_T, \zeta, \mu) &\equiv \int \frac{d(\xi \cdot P) d^2\xi_T}{(xP \cdot n)^2 (2\pi)^3} e^{i(xP + p_T) \cdot \xi} \left\langle P \left| F_a^{n\nu}(0) \left(\mathcal{U}_{[0,\xi]}^{n[-]} \right)_{ab} F_b^{n\mu}(\xi) \right| P \right\rangle \Big|_{\xi \cdot P' = 0} \\ &= -\frac{1}{2x} \left\{ g_T^{\mu\nu} f_1^g(x, \mathbf{p}_T^2, \zeta, \mu) - \left(\frac{p_T^\mu p_T^\nu}{M_p^2} + g_T^{\mu\nu} \frac{\mathbf{p}_T^2}{2M_p^2} \right) h_1^{\perp g}(x, \mathbf{p}_T^2, \zeta, \mu) \right\}, \end{aligned} \quad (2)$$

with $p_T^2 = -\mathbf{p}_T^2$ and $g_T^{\mu\nu} = g^{\mu\nu} - P^\mu P^\nu / P \cdot P' - P'^\mu P^\nu / P \cdot P'$, where P and P' are the momenta of the colliding protons and M_p their mass. The gauge link $\mathcal{U}_{[0,\xi]}^{n[-]}$ for this process arises from initial state interactions. It runs from 0 to ξ via minus infinity along the direction n , which is a time-like dimensionless four-vector with no transverse components such that $\zeta^2 = (2n \cdot P)^2 / n^2$. With the appropriate choice of ζ and μ , the usual soft factors in Eqs. (1) and (2) are absorbed into the TMD correlators^{22,24} and the hard part is free of large logs. The second line of Eq. (2) contains the parametrization²⁵ of the leading twist contributions to the TMD correlator, where f_1^g is the unpolarized gluon distribution and $h_1^{\perp g}$ the linearly polarized gluon distribution.

The general structure of the differential cross section follows from Eq. (1) and (2) and can be written as²⁶

$$\begin{aligned} \frac{d\sigma}{dQ dY d^2\mathbf{q}_T d\cos\theta d\phi} &\propto F_1 \mathcal{C} [f_1^g f_1^g] + F_2 \mathcal{C} \left[w_2 h_1^{\perp g} h_1^{\perp g} \right] + F_3 \mathcal{C} \left[w_3 f_1^g h_1^{\perp g} + (x_1 \leftrightarrow x_2) \right] \cos(2\phi) \\ &\quad + F_3' \mathcal{C} \left[w_3 f_1^g h_1^{\perp g} - (x_1 \leftrightarrow x_2) \right] \sin(2\phi) + F_4 \mathcal{C} \left[w_4 h_1^{\perp g} h_1^{\perp g} \right] \cos(4\phi), \end{aligned} \quad (3)$$

up to corrections that are \mathbf{q}_T^2/Q^2 suppressed at small \mathbf{q}_T . The cross section is differential in Q , Y and \mathbf{q}_T , which are the invariant mass, rapidity and transverse momentum of the pair in the lab frame and in the Collins-Soper angles θ and ϕ . The latter two are defined as the polar and azimuthal angle in the Collins-Soper frame²⁷, which is the diphoton rest frame with the $\hat{x}\hat{z}$ -plane spanned by the 3-momenta of the colliding protons and the \hat{x} -axis set by their bisector. The convolution \mathcal{C} is defined as

$$\mathcal{C}[w f g] \equiv \int d^2\mathbf{p}_T \int d^2\mathbf{k}_T \delta^2(\mathbf{p}_T + \mathbf{k}_T - \mathbf{q}_T) w(\mathbf{p}_T, \mathbf{k}_T) f(x_1, \mathbf{p}_T^2) g(x_2, \mathbf{k}_T^2), \quad (4)$$

in which the longitudinal momentum fractions are given in the aforementioned kinematical variables by $x_{1,2} = e^{\pm Y} \sqrt{(Q^2 + \mathbf{q}_T^2)/s}$. The weights in the convolutions are defined as

$$\begin{aligned} w_2 &\equiv \frac{2(\mathbf{k}_T \cdot \mathbf{p}_T)^2 - \mathbf{k}_T^2 \mathbf{p}_T^2}{4M_p^4}, & w_3 &\equiv \frac{\mathbf{q}_T^2 \mathbf{k}_T^2 - 2(\mathbf{q}_T \cdot \mathbf{k}_T)^2}{2M_p^2 \mathbf{q}_T^2}, \\ w_4 &\equiv 2 \left[\frac{\mathbf{p}_T \cdot \mathbf{k}_T}{2M_p^2} - \frac{(\mathbf{p}_T \cdot \mathbf{q}_T)(\mathbf{k}_T \cdot \mathbf{q}_T)}{M_p^2 \mathbf{q}_T^2} \right]^2 - \frac{\mathbf{p}_T^2 \mathbf{k}_T^2}{4M_p^4}. \end{aligned} \quad (5)$$

Using the following parametrization of the $X_{0,2}\gamma\gamma$ interaction vertex,

$$\begin{aligned} V[X_0 \rightarrow V^\mu(q_1)V^\nu(q_2)] &= a_1 q^2 g^{\mu\nu} + a_3 \epsilon^{q_1 q_2 \mu\nu}, \\ V[X_2^{\alpha\beta} \rightarrow V^\mu(q_1)V^\nu(q_2)] &= \frac{1}{2} c_1 q^2 g^{\mu\alpha} g^{\nu\beta} + (c_2 q^2 g^{\mu\nu} + c_5 \epsilon^{q_1 q_2 \mu\nu}) \frac{\tilde{q}^\alpha \tilde{q}^\beta}{q^2}, \end{aligned} \quad (6)$$

where $q \equiv q_1 + q_2$ and $\tilde{q} \equiv q_1 - q_2$, one finds for a spin-0 boson up to a constant factor

$$F_1 = (4|a_1|^2 + |a_3|^2)^2, \quad F_2 = (4|a_1|^2 + |a_3|^2)(4|a_1|^2 - |a_3|^2), \quad (7)$$

and for a spin-2 boson

$$\begin{aligned} F_1 &= 18A^+ |c_1|^2 \sin^4 \theta + A^{+2} (1 - 6 \cos^2 \theta + 9 \cos^4 \theta) + 9|c_1|^4 (1 + 6 \cos^2 \theta + \cos^4 \theta), \\ F_2 &= 9A^- |c_1|^2 \sin^4 \theta + A^- A^+ (1 - 6 \cos^2 \theta + 9 \cos^4 \theta), \\ F_3 &= 6B^- [A^+ (3 \cos^2 \theta - 1) + 3|c_1|^2 (\cos^2 \theta + 1)] \sin^2 \theta, \\ F_3' &= 12 \text{Re}(c_1 c_5^*) [A^+ (3 \cos^2 \theta - 1) + 3|c_1|^2 (\cos^2 \theta + 1)] \sin^2 \theta, \\ F_4 &= 18|c_1|^2 [B^+ + 2|c_5|^2] \sin^4 \theta, \end{aligned} \quad (8)$$

where we have defined $A^\pm \equiv |c_1 + 4c_2|^2 \pm 4|c_5|^2$, $B^\pm \equiv |c_1 + 2c_2|^2 \pm 4|c_2|^2$.

3 Numerical results

To make numerical predictions $h_1^{\perp g}$ will be expressed as $h_1^{\perp g} = \mathcal{P} 2M_p^2 / \mathbf{p}_T^2 f_1^g$, where the degree of polarization \mathcal{P} will be calculated as described in an earlier publication²⁸. For f_1^g we use the same Ansatz as described before^{15,29}. Plots are made for the benchmark scenarios commonly used in the literature¹¹, to which we add $2_{h'}^+$, $2_{h''}^+$ and 2_{CPV} . The scenarios are summarized in Table 1.

Table 1: Various spin, parity and coupling scenarios.

	0^+	0^-	2_m^+	2_h^+	$2_{h'}^+$	$2_{h''}^+$	2_h^-	2_{CPV}
a_1	1	0	-	-	-	-	-	-
a_3	0	1	-	-	-	-	-	-
c_1	-	-	1	0	1	1	0	1
c_2	-	-	$-\frac{1}{4}$	1	1	$-\frac{3}{2}$	0	0
c_5	-	-	0	0	0	0	1	5

In Figure 1 we show our predictions for the q_T^2 and CS ϕ distributions. Even parity states have an enhanced cross section at small q_T with respect to negative parity states, but the difference is small with a large uncertainty. Including evolution of the distributions we come to the same conclusion³⁰. To lower the uncertainty, a measurement of the TMDs could be made in a different process, e.g., C even quarkonium production³¹ or C odd quarkonium production in association with a photon³².

The effects are larger on the CS ϕ distribution: various spin-2 coupling scenarios produce non-isotropic ϕ distributions with a modulation of up to 25%. The 2_{CPV} benchmark scenario displays a characteristic *asymmetric* ϕ distribution in the forward region that can *only* be caused by a CP -violating coupling.

4 Conclusions

We have calculated the q_T^2 and CS angle ϕ distribution in the process $pp \rightarrow X_{0,2}X \rightarrow \gamma\gamma X$ using TMD factorization. The q_T^2 distribution depends on the parity of the resonance, but numerical predictions show that the difference is relatively small with a large uncertainty. The

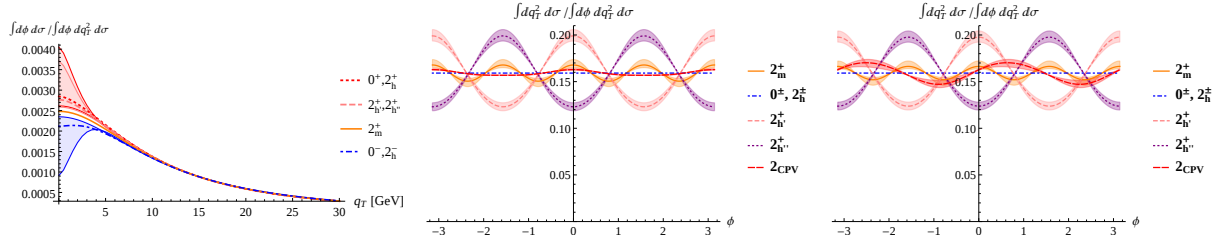


Figure 1 – Plot of the q_T^2 distribution at $Y = 0$ (left), the ϕ distribution at $Y = 0$ (center), and the ϕ distribution at $Y = 1$ (right), all at $\theta = \pi/2$ for a 125 GeV resonance at a center of mass energy of 8 TeV. The shaded area is due to the uncertainty in the degree of polarization.

CS ϕ distribution, on the other hand, shows large modulations, up to 25%, for various spin-2 scenarios, making this a realistic observable to discriminate between spin-0 and various spin-2 scenarios. *This work was supported by the German Bundesministerium für Bildung und Forschung (BMBF), grant no. 05P12VTCTG.*

References

1. G. Aad *et al.* [ATLAS Collaboration], Phys. Lett. B **716**, 1 (2012)
2. S. Chatrchyan *et al.* [CMS Collaboration], Phys. Lett. B **716**, 30 (2012)
3. G. Aad *et al.* [ATLAS Collaboration], Phys. Lett. B **726**, 120 (2013)
4. S. Chatrchyan *et al.* [CMS Collaboration], Phys. Rev. Lett. **110**, 081803 (2013)
5. S. Chatrchyan *et al.* [CMS Collaboration], arXiv:1312.5353 [hep-ex].
6. S. Chatrchyan *et al.* [CMS Collaboration], JHEP **1401**, 096 (2014)
7. S. Chatrchyan *et al.* [CMS Collaboration], arXiv:1401.5041 [hep-ex].
8. S. Chatrchyan *et al.* [CMS Collaboration], Phys. Rev. D **89**, 012003 (2014)
9. S. Y. Choi *et al.*, Phys. Lett. B **553**, 61 (2003)
10. Y. Gao *et al.*, Phys. Rev. D **81**, 075022 (2010)
11. S. Bolognesi *et al.* Phys. Rev. D **86**, 095031 (2012)
12. S. Y. Choi, M. M. Muhlleitner and P. M. Zerwas, Phys. Lett. B **718**, 1031 (2013)
13. J. Ellis, R. Fok, D. S. Hwang, V. Sanz and T. You, Eur. Phys. J. C **73**, 2488 (2013)
14. D. Boer *et al.*, Phys. Rev. Lett. **108**, 032002 (2012)
15. D. Boer *et al.*, Phys. Rev. Lett. **111**, 032002 (2013)
16. C. Balazs *et al.*, Phys. Rev. **D76**, 013008 (2007); Phys. Rev. **D76**, 013009 (2007).
17. S. Catani, M. Grazzini, Nucl. Phys. B **845** (2011) 297.
18. S. Catani and M. Grazzini, Eur. Phys. J. C **72**, 2013 (2012)
19. D. de Florian, G. Ferrera, M. Grazzini and D. Tommasini, JHEP **1111**, 064 (2011)
20. D. de Florian, G. Ferrera, M. Grazzini and D. Tommasini, JHEP **1206**, 132 (2012)
21. S. Catani *et al.*, Nucl. Phys. B **881**, 414 (2014)
22. X. -d. Ji, J. -P. Ma and F. Yuan, JHEP **0507**, 020 (2005)
23. P. Sun, B. -W. Xiao and F. Yuan, Phys. Rev. D **84**, 094005 (2011)
24. J. P. Ma, J. X. Wang and S. Zhao, Phys. Rev. D **88**, 014027 (2013)
25. P. J. Mulders and J. Rodrigues, Phys. Rev. D **63**, 094021 (2001)
26. J. -W. Qiu, M. Schlegel and W. Vogelsang, Phys. Rev. Lett. **107**, 062001 (2011)
27. J. C. Collins and D. E. Soper, Phys. Rev. D **16**, 2219 (1977).
28. W. J. den Dunnen and M. Schlegel, arXiv:1310.4965 [hep-ph].
29. W. J. den Dunnen, arXiv:1311.1048 [hep-ph].
30. D. Boer and W. J. den Dunnen, arXiv:1404.6753 [hep-ph].
31. D. Boer and C. Pisano, Phys. Rev. D **86**, 094007 (2012)
32. W. J. den Dunnen, J. -P. Lansberg, C. Pisano and M. Schlegel, arXiv:1401.7611 [hep-ph].